Contemporary Engineering Sciences, Vol. 3, 2010, no. 6, 269 - 283

Electrical Discharge Machining (EDM) by Using Non-Fourier Heat Conduction Model

Seyfolah Saedodin

Department of Mechanical Engineering, Faculty of Engineering
Semnan University, Semnan, Iran
S_Sadodin@iust.ac.ir

Mohsen Torabi

Department of Mechanical Engineering, Faculty of Engineering
Semnan University, Semnan, Iran
Torabi_mech@yahoo.com

Abstract

Whereas in electrical discharge machining (EDM) the heat flux entering the workpiece is extremely large, the Fourier heat conduction model may fails. The purpose of the present paper is to carry out the non-Fourier effect subjected to heat flux boundary condition in EDM process. The governing equations have been expressed in cylindrical coordinates. Equations are solved by deriving the analytical solution with the method of separation of variables. The temperature layers and profiles of sample calculations show that, it is not acceptable applying the Fourier heat conduction model for estimating the temperature of workpiece. Also It can be perceived that, according the amount of Vernotte number for a specific Fourier number, it is possible that the temperature of different points of workpiece become even lower than initial temperature. Which this fact does not occur by applying Fourier heat conduction model.

Keywords: Electrical Discharge Machining (EDM) – Non-Fourier Heat Conduction – Relaxation Time – Separation of Variables

Nomenclature

$A, B, C, D, a_n, c_1, c_2, C_{12}, C_{fg}$	Constant coefficients		
Bi	Biot number	Ve	Vernotte number
c	Specific heat capacity	$X(\xi), Z(\omega)$	Function employed in Eqs.(17) and (29)
F_c	Fraction of power going to the cathode	**Greek symbols**	
Fo	Fourier number	α	Thermal diffusivity
I	discharge current	ρ	Mass density
k	Thermal conductivity	Δ	Laplace's differential operator
L	Height of the cylinder	∇	Gradient operator
M	Square ratio of height to radius of cylinder	τ	Thermal relaxation time
q_0	Maximum heat flux	θ	Dimensionless temperature
r_1	Radius of heat flux	ξ, ω	Dimensionless spatial coordinate
R	Radius of cylinder	$\psi(\xi, \omega, Fo)$	Function employed in Eq. (12)
R_{pc}	spark radius	$\phi(\xi, \omega)$	Function employed in Eq. (12)
r, z	Spatial coordinate	ξ_1	Dimensionless radius of heat flux
t	Temporal coordinate	$\beta_n, \gamma_f, \eta_g$	Eigenvalues
T	Temperature	κ	Parameter difinded by Eq. (42a)
$T(Fo)$	Function employed in Eq. (29)	κ_i	Parameter difinded by Eq. (42b)
T_i	Initial temperature	ϑ_l	Parameter difinded by Eq. (40)
T_∞	Ambient temperature		
V	discharge voltage		

1. Introduction

Electrical discharge machining (EDM) is a non-traditional concept of machining which has been widely used to produce dies and molds [8]. This high technology is developed in the late 1940s [14], which supports about 7% of all machine tool sales in the world [11]. Its method is defined as removing materials from a part by means of a series of repeated electrical discharges between tool called the electrode and the work piece in the presence of a dielectric fluid [6]. The maximum heat q_0 entering the workpiece due to EDM spark is represented by [4]

$$q_0 = \frac{4.56 F_c V I}{\pi R_{pc}^2} \tag{1}$$

Where F_c is the fraction of total EDM spark power going to the cathode; V is the discharge voltage (V); I is the discharge current (A); R_{pc} is the spark radius (μm) at the workpiece surface. It can be perceived from simple calculation that, the heat flux entering the workpiece in EDM process can be more than $10^{11} wm^{-2}$. So, if we want to predict the temperature of workpiece during the EMD process, Fourier heat conduction model cannot be applied [7].

In order to eliminate these fails, Cattaneo [3] and Vernotte [16], independently proposed a modification of Fourier's law. Which, is now well known as Cattaneo-Vernotte's constitutive equation

$$\mathbf{q} + \tau \frac{\partial \mathbf{q}}{\partial t} = -k \nabla T \tag{2}$$

Where $\mathbf{q}$ is the heat flux vector, τ is the thermal relaxation time, k is the constant thermal conductivity of the material and ∇T is the temperature gradient. If equation (2), combined with the conservation of energy gives the non-Fourier heat conduction equation

$$\frac{\partial T}{\partial t} + \tau \frac{\partial^2 T}{\partial t^2} = \alpha \Delta T \tag{3}$$

Where $\alpha = \frac{k}{\rho c}$, ρ, c and Δ are thermal diffusivity, mass density, specific heat capacity and Laplace's differential operator, respectively. Equation (3) is a hyperbolic partial differential equation and causes the propagation speed, reach a limit amount $\sqrt{\alpha/\tau}$, in $\tau > 0$.

There are many analytical solutions of non-Fourier heat conduction. Most researches applied non-Fourier heat conduction model in one-dimensional. Lewandowska and Malinowski [5] solved the case of a thin film subjected to a symmetrical heating on both side. Moosaie investigated the non-Fourier heat conduction model in a finite medium with the arbitrary source term [9] and arbitrary initial condition [10]. Tang and Araki [15] computed the non-Fourier fin problems under the periodic thermal conditions. Zhang et al. [17] presented a non-Fourier heat conduction model with heat source. Saleh and Al-Nimr [13] employed Laplace transforms, software package MATLAP and Taylor series, to solve the one-dimensional non-Fourier heat conduction model. To the authors' knowledge, there is only one paper that solved multi-dimensional non-Fourier heat conduction model analytically. Barletta and Zanchini [1] analytically investigated the non-Fourier heat conduction model using three-dimensional rectangular coordinates. In this paper an analytical expression of temperature field is obtained for a cylindrical workpiece in EDM process. Both non-Fourier and Fourier heat conduction equations have been solved in cylindrical coordinates. In fact, the solution of the problem is obtained by employing the method

of separation of variables. Using our analytical solution, we performed sample calculation of temperature surfaces and profiles for workpiece.

2. Problem statement

Due to the random and complex nature of EDM, the following assumptions are made to make the problem mathematically tractable.

2.1. Assumptions

1. The domain is considered as axisymmetric.
2. The workpiece material is homogeneous and isotropic.
3. The material properties of the workpiece are temperature independent.
4. The heat transfer to the workpiece is by conduction.

2.2. Thermal model

Have analyzed this problem by considering the heat flux profile of EDM process is disc type. Consider a cylinder, as shown as Fig. 1. The heat flux due to EDM spark is applied normally to the upper surface ($Z = L$) of the cylinder but only for $r < r_1$.

2.2.1. Governing differential equation

For this case, the non-Fourier heat conduction equation without any heat generation, the governing equation can then be expressed as:

$$\frac{1}{\alpha}\frac{\partial T}{\partial t} + \frac{\tau}{\alpha}\frac{\partial^2 T}{\partial t^2} = \frac{\partial^2 T}{\partial r^2} + \frac{1}{r}\frac{\partial T}{\partial r} + \frac{\partial^2 T}{\partial z^2} \tag{4}$$

2.2.2. Boundary conditions

Consider underneath surface ($Z = 0$) has been at temperature of dielectric fluid and sidelong surface transfer the heat with dielectric fluid. For this case the boundary conditions are:

$$\frac{\partial T}{\partial r}(0, z, t) = 0 \tag{5a}$$

$$k\frac{\partial T}{\partial r}(R, z, t) + h[T(R, z, t) - T_\infty] = 0 \tag{5b}$$

$$T(r, 0, t) = T_\infty \tag{5c}$$

$$k\frac{\partial T}{\partial z}(r, L, t) = \begin{cases} q & r < r_1 \\ 0 & r > r_1 \end{cases} \tag{5d}$$

2.2.3. Initial conditions

Consider the solid initially has been at the temperature of dielectric fluid. Then:

$$T_i = T_\infty \tag{6}$$

Hence the initial conditions are:

$$T(r,z,0)=T_\infty \tag{7a}$$

$$\frac{\partial T}{\partial t}(r,z,0)=0 \tag{7b}$$

3. Analytical solution

For convenience of subsequent analysis, we introduce the following dimensionless quantities:

$$\theta=k\frac{T-T_\infty}{Lq},\qquad \xi=\frac{r}{R},\qquad \omega=\frac{z}{L},\qquad Fo=\frac{\alpha t}{L^2},$$
$$Ve=\sqrt{\frac{\alpha\tau}{L^2}},\qquad M=(\frac{L}{R})^2,\qquad \xi_1=\frac{r_1}{R},\qquad Bi=\frac{hR}{k} \tag{8}$$

Where θ is dimensionless temperature and ξ,ω are dimensionless coordinates. Fo is the Fourier number and Ve is the Vernotte number, M is Square ratio of height to radius of cylinder, ξ_1 is dimensionless radius of heat flux and Bi is the Biot number. By introducing the dimensionless quantities, we expressed non-Fourier heat conduction model as:

$$Ve^2\frac{\partial^2\theta}{\partial Fo^2}+\frac{\partial\theta}{\partial Fo}=M\frac{\partial^2\theta}{\partial\xi^2}+\frac{M}{\xi}\frac{\partial\theta}{\partial\xi}+\frac{\partial^2\theta}{\partial\omega^2} \tag{9}$$

Also, the boundary conditions are:

$$\frac{\partial\theta}{\partial\xi}(0,\omega,Fo)=0 \tag{10a}$$

$$\frac{\partial\theta}{\partial\xi}(1,\omega,Fo)+Bi\theta(1,\omega,Fo)=0 \tag{10b}$$

$$\theta(\xi,0,Fo)=0 \tag{10c}$$

$$\frac{\partial\theta}{\partial\omega}(\xi,1,Fo)=\begin{cases}1 & \xi\le\xi_1\\ 0 & \xi>\xi_1\end{cases} \tag{10d}$$

and the initial conditions are:

$$\frac{\partial\theta}{\partial Fo}(\xi,\omega,0)=0 \tag{11a}$$

$$\theta(\xi,\omega,0)=0 \tag{11b}$$

If we want to apply the well-known separation of variables method, first we should split up eq. (9) with the boundary (10) and the initial conditions (11) into a set of simpler problems. Carslaw and Jaeger [2] and Özisik [12] determined the solution of Eq. (9) from:

$$\theta(\xi,\omega,Fo)=\psi(\xi,\omega,Fo)+\phi(\xi,\omega) \tag{12}$$

Where the temperature $\phi(\xi,\omega)$ is taken as the solution of the following Eqs.:

$$M\frac{\partial^2\phi}{\partial\xi^2}+\frac{M}{\xi}\frac{\partial\phi}{\partial\xi}+\frac{\partial^2\phi}{\partial\omega^2}=0 \tag{13}$$

$$\frac{\partial}{\partial\xi}\phi(0,\omega)=0 \tag{14a}$$

$$\frac{\partial}{\partial\xi}\phi(1,\omega)+Bi\phi(1,\omega)=0 \tag{14b}$$

$$\phi(\xi,0)=0 \tag{14c}$$

$$\frac{\partial}{\partial\omega}\phi(\xi,1)=\begin{cases}1 & \xi\le\xi_1\\ 0 & \xi>\xi_1\end{cases} \tag{14d}$$

Where the temperature $\psi(\xi,\omega,Fo)$ is taken as the solution of the following Eqs.:

$$Ve^2\frac{\partial^2\psi}{\partial Fo^2}+\frac{\partial\psi}{\partial Fo}=M\frac{\partial^2\psi}{\partial\xi^2}+\frac{M}{\xi}\frac{\partial\psi}{\partial\xi}+\frac{\partial^2\psi}{\partial\omega^2} \tag{15}$$

$$\frac{\partial}{\partial\xi}\psi(0,\omega,Fo)=0 \tag{16a}$$

$$\frac{\partial}{\partial\xi}\psi(1,\omega,Fo)+Bi\,\psi(1,\omega,Fo)=0 \tag{16b}$$

$$\psi(\xi,0,Fo)=0 \tag{16c}$$

$$\frac{\partial}{\partial\omega}\psi(\xi,1,Fo)=0 \tag{16d}$$

$$\frac{\partial}{\partial Fo}\psi(\xi,\omega,0)=0 \tag{16e}$$

$$\psi(\xi,\omega,0)=-\phi(\xi,\omega) \tag{16f}$$

Solving the partial differential equation (13), we should use the following separation ansantz:

$$\phi(\xi,\omega)\equiv X(\xi)Z(\omega) \tag{17}$$

By substituting eq. (17) into eq. (13) and subtracting to (17):

$$M\left(\frac{1}{X}\frac{d^2X}{d\xi^2}+\frac{1}{X\xi}\frac{dX}{d\xi}\right)=-\frac{1}{Z}\frac{d^2Z}{d\omega^2}=\pm\beta^2 \tag{18}$$

Here $-\beta^2$ is suitable to our problem. Finally, the problem separately expressed in ξ- and ω-directions as follows:

$$\frac{d^2X}{d\xi^2}+\frac{1}{\xi}\frac{dX}{d\xi}+m^2X=0 \tag{19}$$

$$\frac{d}{d\xi}X(0)=0 \tag{20a}$$

$$\frac{d}{d\xi}X(1)+BiX(1)=0 \tag{20b}$$

$$\frac{d^2Z}{d\omega^2}-\beta^2Z=0 \tag{21}$$

$$Z(0)=0 \tag{22}$$

Where

$$m^2 = \frac{\beta^2}{M} \tag{23}$$

By solving Eqs. (19) and (21) according to conditions (20) and (22):

$$X(\xi) = A\,\mathrm{J}_0(\xi m_n) \tag{24}$$

$$Z(\omega) = B\sinh(\beta_n \omega) \tag{25}$$

Where β_n is eigenvalue of Eq. $Bi\,\mathrm{J}_0(\frac{\beta_n}{\sqrt{M}}) - \frac{\beta_n}{\sqrt{M}}\mathrm{J}_1(\frac{\beta_n}{\sqrt{M}}) = 0$. The first eight eigenvalues of this Eq. are given in Table 1 for $Bi = 2$ and $M = 16$. By substituting the Eqs. (24) and (25) into Eq. (17), we obtain following Eq. as the solution of the Eq. (13):

$$\phi(\xi, \omega) = \sum_{n=1}^{\infty} a_n \sinh(\beta_n \omega)\,\mathrm{J}_0(m_n \xi) \tag{26}$$

Using boundary condition (13d) and orthogonality condition, we find the following Eq.:

$$a_n \beta_n \cosh\beta_n = \frac{\int_0^{\xi_1} \xi\,\mathrm{J}_0(m_n \xi)\,d\xi}{\int_0^1 \xi\,\mathrm{J}_0{}^2(m_n \xi)\,d\xi} \tag{27}$$

Finally, the constant a_n is given as following Eq.:

$$a_n = \frac{2\xi_1\,\mathrm{J}_1(\frac{\beta_n}{\sqrt{M}}\xi_1)}{\sqrt{M}\cosh\beta_n[\mathrm{J}_0(\frac{\beta_n}{\sqrt{M}})]^2 \times [Bi^2 + \frac{\beta_n{}^2}{M}]} \tag{28}$$

Table 1. First eight values of β_n								
n	1	2	3	4	5	6	7	8
β	6.3977	17.1638	29.1535	41.4633	53.8875	66.3641	78.8688	91.3902

To solve the partial differential equation (15), we should use the following separation ansantz:

$$\psi(\xi, \omega, Fo) \equiv X(\xi)Z(\omega)T(Fo) \tag{29}$$

By substituting the Eq. (29) into the Eq. (15) and subtracting to (29):

$$\frac{Ve^2}{T}\frac{d^2T}{dFo^2} + \frac{1}{T}\frac{dT}{dFo} = M(\frac{1}{X}\frac{d^2X}{d\xi^2} + \frac{1}{X\xi}\frac{dX}{d\xi}) + \frac{1}{Z}\frac{d^2Z}{d\omega^2} = \pm\eta^2 \tag{30}$$

Here $-\eta^2$ is suitable to our problem. Finally, the problem separately expressed in ξ- and ω- and Fo-directions as follows:

$$\frac{d^2Z}{d\omega^2}+\eta^2 Z=0 \tag{31}$$

$$Z(0)=0 \tag{32a}$$

$$\frac{\partial}{\partial\omega}Z(1)=0 \tag{32b}$$

$$\frac{d^2X}{d\xi^2}+\frac{1}{\xi}\frac{dX}{d\xi}+\frac{\gamma^2}{M}X=0 \tag{33}$$

$$\frac{d}{d\xi}X(0)=0 \tag{34a}$$

$$\frac{d}{d\xi}X(1)+BiX(1)=0 \tag{34b}$$

$$Ve^2\frac{d^2T}{dFo^2}+\frac{dT}{dFo}+(\eta^2+\gamma^2)T=0 \tag{35}$$

$$\frac{d}{dFo}T(0)=0 \tag{36}$$

Solving the Eqs. (31), (33) and (35) according to conditions (32), (34) and (36):

$$Z(\omega)=C\sin(\eta_g\omega) \tag{37}$$

$$X(\xi)=D\,\mathrm{J}_0(\frac{\gamma_f}{\sqrt{M}}\xi) \tag{38}$$

Where η_g and γ_k are eigenvalues of Eqs. $\cos\eta_g=0$ and $Bi\,\mathrm{J}_0(\frac{\gamma_f}{\sqrt{M}})-\frac{\gamma_f}{\sqrt{M}}\mathrm{J}_1(\frac{\gamma_f}{\sqrt{M}})=0$, respectively. For the Eq. (35), if $1-4Ve^2\vartheta_l^{\,2}>0$, we obtain:

$$T(Fo)=e^{-\frac{Fo}{2Ve^2}}(c_1\sinh(\frac{\kappa Fo}{2Ve^2})+c_2\cosh(\frac{\kappa Fo}{2Ve^2})) \tag{39}$$

Where

$$\vartheta_l^{\,2}=\lambda_f^{\,2}+\eta_g^{\,2} \tag{40}$$

And if $1-4Ve^2\vartheta_l^{\,2}<0$

$$T(Fo)=e^{-\frac{Fo}{2Ve^2}}(c_1\sin(\frac{\kappa_i Fo}{2Ve^2})+c_2\cos(\frac{\kappa_i Fo}{2Ve^2})) \tag{41}$$

Where

$$\kappa=\sqrt{1-4Ve^2\vartheta_l^{\,2}} \tag{42a}$$

$$\kappa=i\kappa_i \tag{42b}$$

By substituting the Eqs. (39) and (41) into initial condition (36) to eliminating c_1 or c_2:

$$T(Fo)=C_{12}\begin{cases} e^{-\frac{Fo}{2Ve^2}}\left\{\frac{1}{\kappa}\sinh(\frac{\kappa Fo}{2Ve^2})+\cosh(\frac{\kappa Fo}{2Ve^2})\right\} & \kappa=real \\ e^{-\frac{Fo}{2Ve^2}}\left\{\frac{1}{\kappa_i}\sin(\frac{\kappa_i Fo}{2Ve^2})+\cos(\frac{\kappa_i Fo}{2Ve^2})\right\} & \kappa=i\kappa_i \end{cases} \tag{43}$$

Substituting the Eqs. (37), (38) and (43) into (29), the following equation for $\psi(\xi,\omega,Fo)$ obtain:

$$\psi(\xi,\omega,Fo)=\sum_{f=1}^{F}\sum_{g=0}^{G}C_{fg}\exp(-\frac{Fo}{2Ve^2})\times\left[\frac{1}{\kappa}\sinh(\frac{\kappa Fo}{2Ve^2})+\cosh(\frac{\kappa Fo}{2Ve^2})\right]\sin(\eta_g\omega)J_0(\frac{\gamma_f}{\sqrt{M}}\xi)$$
$$+\sum_{F+1}^{\infty}\sum_{G+1}^{\infty}C_{fg}\exp(-\frac{Fo}{2Ve^2})\left[\frac{1}{\kappa_i}\sin(\frac{\kappa_i Fo}{2Ve^2})+\cos(\frac{\kappa_i Fo}{2Ve^2})\right]\sin(\eta_g\omega)J_0(\frac{\gamma_f}{\sqrt{M}}\xi) \tag{44}$$

Where F,G are maximum value of f,g when the κ is real for each loop, respectively. Using boundary condition (16f) and orthogonality condition, we find the following Eq.:

$$C_{fg}=\frac{-a_f\int_0^1\sinh(\gamma_f\omega)\sin(\eta_g\omega)d\omega}{\int_0^1\sin^2(\eta_g\omega)d\omega} \tag{45}$$

Finally

$$C_{fg}=-4\frac{\xi_1 J_1(\frac{\gamma_f}{\sqrt{M}}\xi_1)\gamma_f}{\sqrt{M}[J_0(\frac{\gamma_f}{\sqrt{M}})]^2\times[Bi^2+\frac{\gamma_f^2}{M}]}\frac{(-1)^g}{(\eta_g^2+\gamma_f^2)} \tag{46}$$

As a good comparison, we should solve the same problem with Fourier model. If Fourier's law holds, i.e. in the limit $Ve\to 0$, the values of κ_i are always real and therefore, $\psi(\xi,\omega,Fo)$ becomes

$$\psi(\xi,\omega,Fo)=\sum_{f=1}^{\infty}\sum_{g=0}^{\infty}C_{fg}\exp(-\vartheta_l^2 Fo)\sin(\eta_g\omega)J_0(\frac{\gamma_f}{\sqrt{M}}\xi) \tag{47}$$

4. Result and discussion

Using our analytical solution, we performed sample numerical computations of temperature surfaces and profiles in the cylinder for the disc type of the heat source, based on Eqs. (12), (26), (44) and (47). These calculations are obtained for $\xi_1=0.2$, $Bi=2$ and $M=16$. The results of calculations are presented in Figs. 2-5.

4.1. Comparison of surface temperature evolvement obtained from Fourier and non-Fourier model with same Fourier number

Fig. 2 and 3 show the surface temperature profiles for the two cases. The Fourier number and Vernotte number that we simulated for are 0.5 and 0.7, respectively. It can be perceived from Fig. 2 that, in Fourier model the speed of propagation is infinite. At the moment, all of the workpiece can touch the heat flux. Also, it can be perceived from Fig. 3 that, because of the non-Fourier effect, the heat wave cannot touch the other side of the workpiece at the moment and due to the non-Fourier effects, heat waves can be seen clearly in Fig. 3. As seen in Figs. 2 and 3 the nature of Fourier model and non-Fourier model are completely different and the amount of temperature from these two are not the same.

4.2. Comparison of temperature distribution for non-Fourier model with same Fourier number but at different Vernotte number along the ω direction

Fig. 4 shows temperature profiles along the ω direction at $Fo = 0.5$ and $\xi = 0$ in cylinder for the disc type of the heat source. This Fig. shows that, according the amount of Vernotte number for a specific Fourier number, it is possible that the temperature of different points of workpiece become even lower than initial temperature. Also, it can be seen that due to the non-Fourier effects, the temperature of lots of points in the workpiece remain steady for some moments. It is noticeable that, if Fourier model has been applied, the temperature of all points of the workpiece become higher than initial temperature.

4.3. Comparison of temperature distribution for the non-Fourier model with different Vernotte number for the unique point

Fig. 5 shows temperature profiles at the point $\xi = 0$ and $\omega = 0.5$. It can be seen from Fig. 5 that, the higher Vernotte number causes each point to be at initial temperature, more and the point can get to higher temperature during the process. Previous effect can be generalized in all of the workpiece's points. As it is observed, as much as the Vernotte number increases, the Fourier number that the considered point or totally the whole cylinder needs, in order to reach the equilibrium temperature, increases. Regarding Fig. 5, the thermal wave reflection causes the existence of a fracture in the thermal profile of the point and it can be seen that, due to the reflection of heat waves, the temperature of a specific point can become several times lower than initial temperature and this fact is very important to estimate the thermal stress of workpiece. Also, it can be concluded that, the amount of thermal relaxation time is so important to predict the temperature of workpiece during EDM process.

5. Conclusion

In this paper, the two-dimensional non-Fourier heat conduction model was solved analytically for the cylinderical workpiece in EDM process by the separation of variables method. Three different examples have been analyzed. We concluded that, calculating the thermal relaxation time is important to predict the temperature of workpiece during EDM process. Also, it can be seen that, the more the Vernotte number, the more the Foureir number passed for the point that can feel the thermal wave. We also perceived that, the more the Vernotte number, the more the Fourier number need for the workpiece to reach an equilibrium temperature. Finally, we observed that, applying the Fourier heat conduction model instead of non-Fourier model for predicting the temperature of workpiece during EDM process has significant differences.

Acknowledgment

The authors gratefully acknowledge the support of the department of mechanical engineering and the office of gifted of Semnan University for funding the current research grant.

References

[1] A. Barletta, E. Zanchini, Three-dimensional propagation of hyperbolic thermal waves in a solid bar with rectangular cross-section, International Journal of Heat and Mass Transfer 42 (1999) 219-229.

[2] H. S. Carslaw and J. C. Jaeger, Conduction of Heat in Solids, 2nd ed., Oxford University Press, New York, 2000, Chap. 1.

[3] C. Cattaneo, Sur une forme de l'équation de la chaleur éliminant le paradoxe d'une propagation instantanée, C.R. Acad. Sci. 247 (4) (1958) 431–433.

[4] S. N. Joshi, S. S. Pande, Development of an intelligent process model for EDM, Int J Adv Manuf Technol 45 (2009) 300–317.

[5] M. Lewandowska, L. Malinowski, An analytical solution of the hyperbolic heat conduction equation for the case of a finite medium symmetrically heated on both sides, International Communications in Heat and Mass Transfer 33 (2006) 61– 69.

[6] C. J. Luis, I. Puertas, G. Villa, Material removal rate and electrode wear study on the EDM of silicon carbide, Journal of Materials Processing Technology 164–165 (2005) 889–896.

[7] M. J. Maurer, H. A. Thompson, Non-Fourier Effects at High Heat Flux, Journal of Heat Transfer, 95 (1973) 284-286.

[8] N. Mohd Abbas, Darius G. Solomon, Md. Fuad Bahari, A review on current research trends in electrical discharge machining (EDM), International Journal of Machine Tools & Manufacture 47 (2007) 1214–1228.

[9] A. Moosaie, Non-Fourier heat conduction in a finite medium with arbitrary source term and initial conditions, Forsch. Ing.wes. 71 (2007) 163–169.

[10] A.Moosaie, Non-Fourier heat conduction in a finite medium with insulated boundaries and arbitrary initial conditions, International Communications in Heat and Mass Transfer 35 (2008) 103–111.

[11] H. Moser, Growth industries rely on EDM, Manuf. Eng. 127 (2001) 62–68.

[12] M. N. Ozisik, Heat conduction, 2nd ed., John Wiley &Sons, New York, 1993, Chap. 2.

[13] A. Saleh, M. Al-Nimr, Variational formulation of hyperbolic heat conduction problems applying Laplace transform technique, International Communications in Heat and Mass Transfer 35 (2008) 204–214.

[14] S. Singh, S. Maheshwari, P.C. Pandey, Some investigations into the electric discharge machining of hardened tool steel using different electrode materials, Journal of Materials Processing Technology 149 (2004) 272–277.

[15] D.W. Tang, N. Araki, Non-Fourier heat conduction in a finite medium under periodic surface thermal disturbance, International Journal of Heat and Mass Transfer 39 (8) (1996) 1585–1590.

[16] P. Vernotte, Les paradoxes de la théorie continue de l'équation de la chaleur, C.R. Acad. Sci. 246 (22) (1958) 3154–3155.

[17] Duanming Zhang, Li Li, Zhihua Li, Li Guan, Xinyu Tan, Non-Fourier conduction model with thermal source term of ultra short high power pulsed laser ablation and temperature evolvement before melting, Physica B 364 (2005) 285–293.

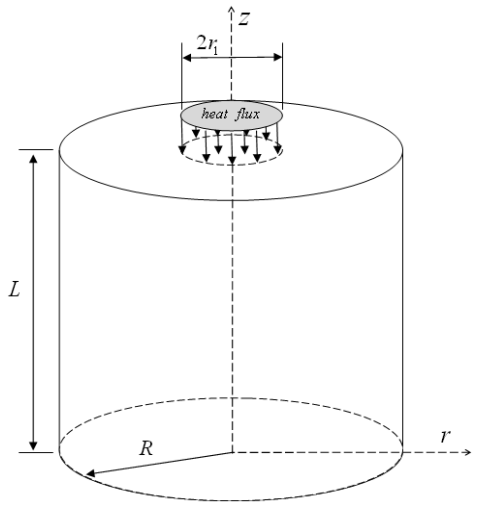

Fig. 1. The cylinder configuration

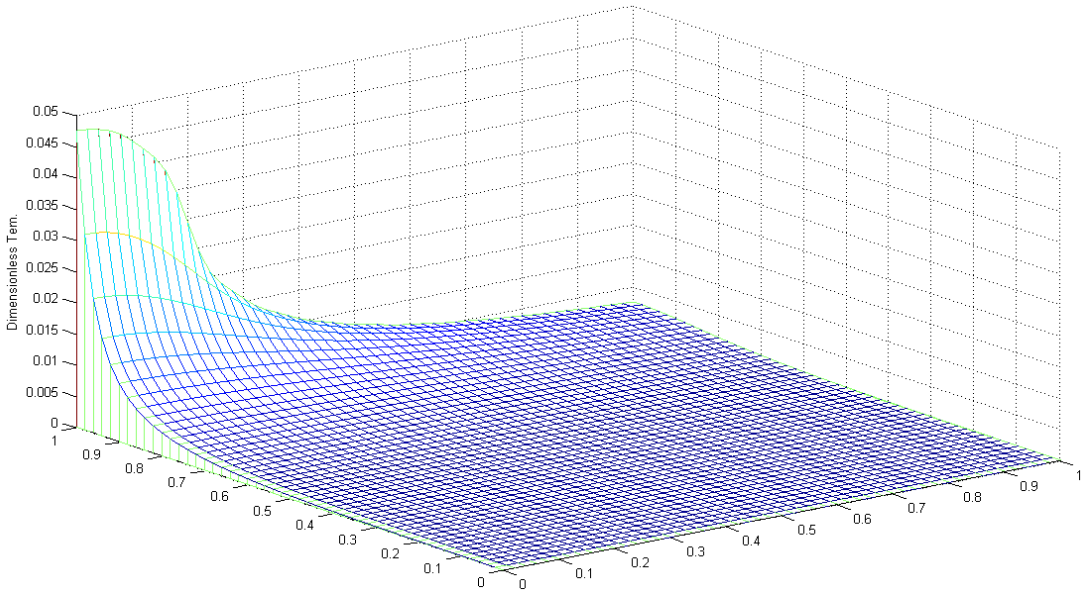

Fig. 2. The surface temperature evolution with $Fo = 0.5$ for Fourier model

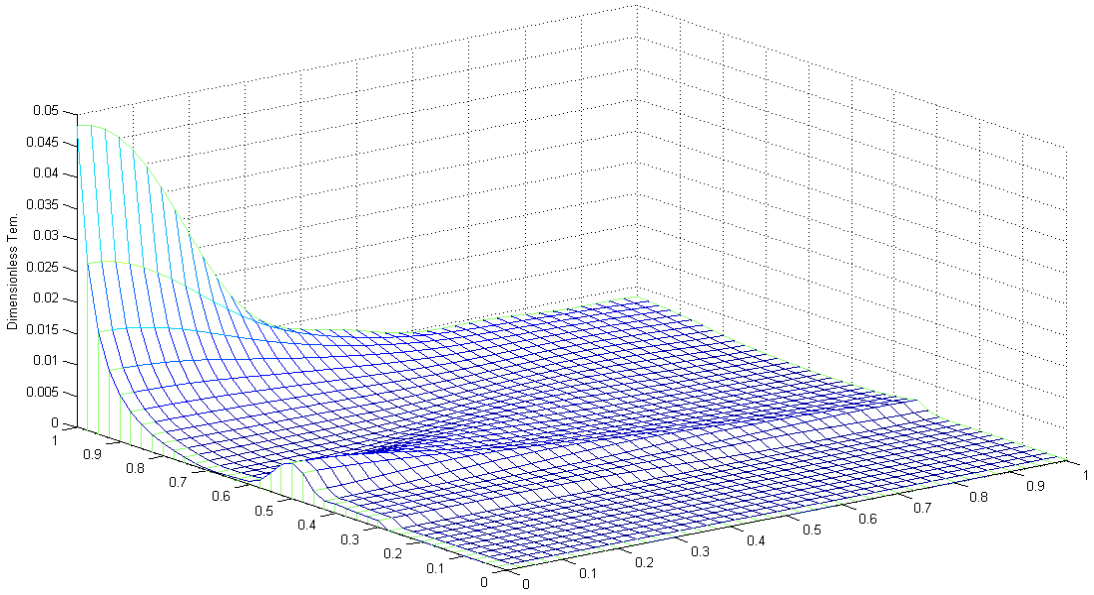

Fig. 3. The surface temperature evolution with $Fo = 0.5$ and $Ve = 0.7$ for non-Fourier model

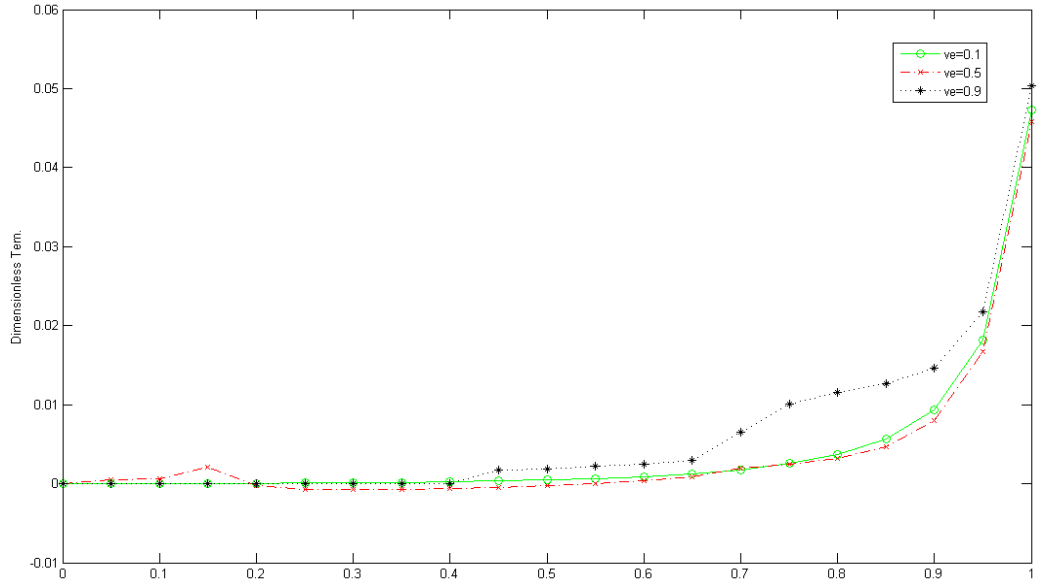

Fig. 4. The temperature distribution for the non-Fourier model with the same Fourier number, but at different Vernotte number along the ω direction

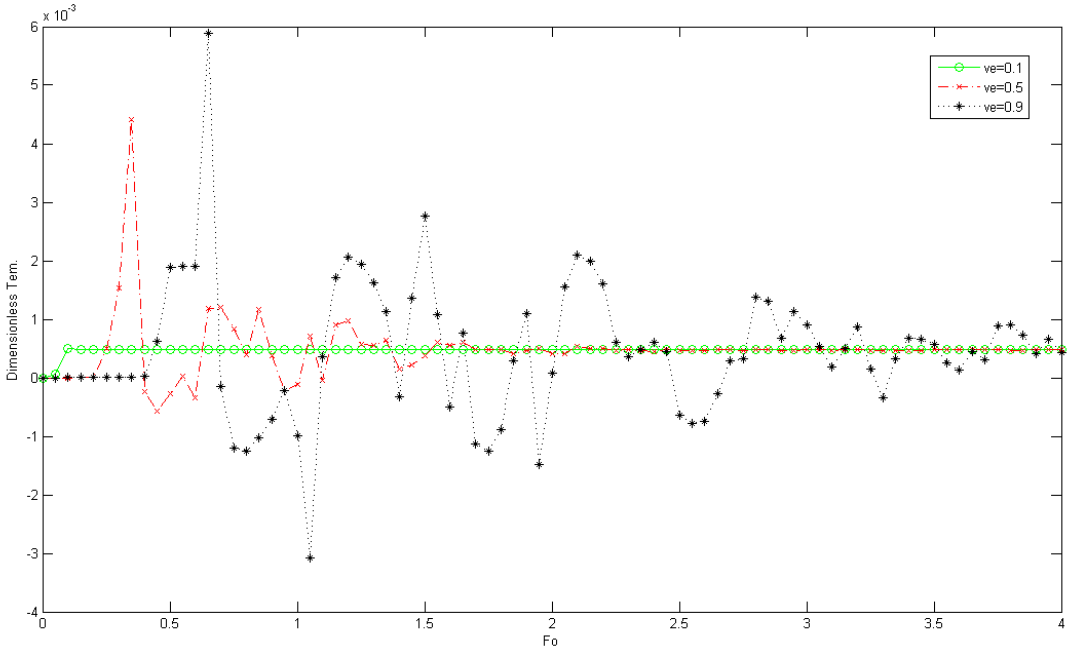

Fig. 5. The temperature distribution for non-Fourier model with different Vernotte number for the unique point

Received: May, 2010